ISCI, Volume *22*

Supplemental Information

Regenerative Adaptation to Electrochemical Perturbation in Planaria: A Molecular Analysis of Physiological Plasticity

Maya Emmons-Bell, Fallon Durant, Angela Tung, Alexis Pietak, Kelsie Miller, Anna Kane, Christopher J. Martyniuk, Devon Davidian, Junji Morokuma, and Michael Levin

Supplemental Information

Supplemental Figures

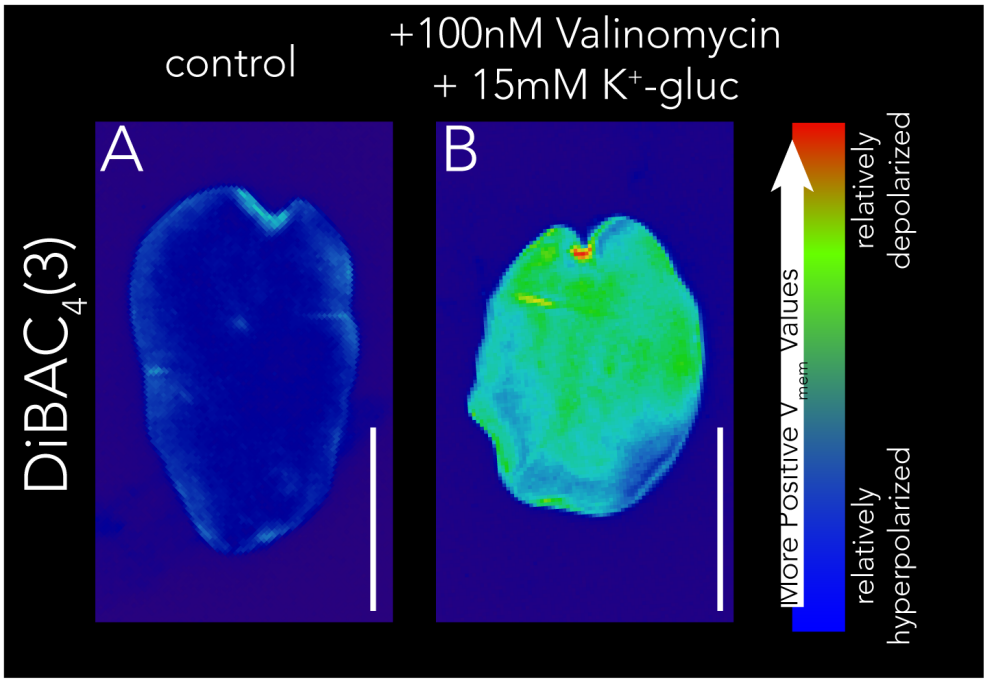

Figure S1. Valinomycin and potassium gluconate-induced depolarization can be visualized with $DiBAC_4(3)$, Related to Figure 3. Pretail fragments (fragments that contain the trunk region of the worm posterior to the pharynx and anterior to the tail) of *Dugesia japonica* were cut and placed into vehicle (**A**) or 100nM Valinomycin + 15mM potassium gluconate (K^+-gluc) (**B**) for 1 hour, then mounted and imaged. Both Valinomycin and K^+-gluc were used to optimize depolarization. Images were taken of ventral surface of fragment and were far-field and dark-field corrected. Images are pseudocolored to allow for ease of visualization of depolarization patterns, but worms were imaged in the same frame so as not to confound data after pseudocoloring, and all image analysis was done using raw images. Scale bars 0.5mm.

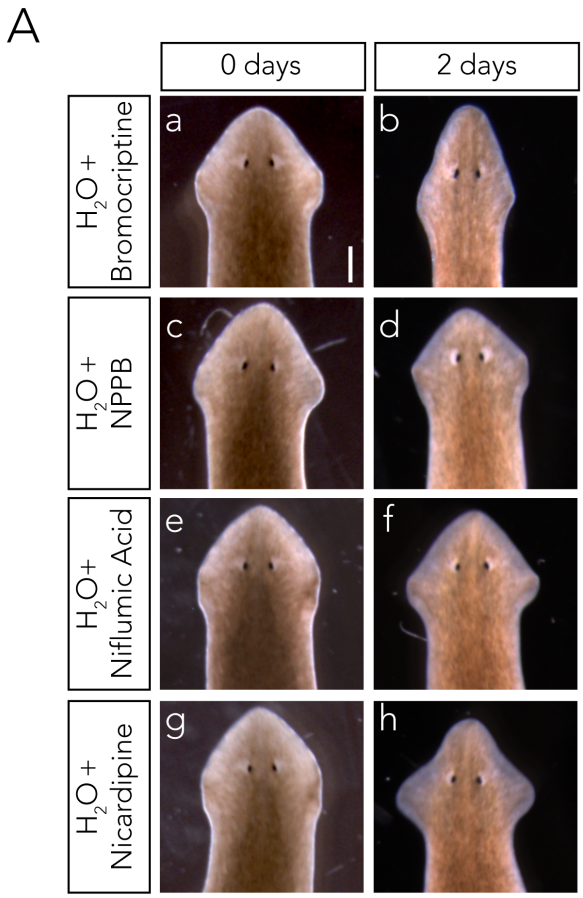

Figure S2. Drug treatment alone does not affect planaria, Related to Figure 4. (**A**) Exposure to Bromocriptine (**a**,**b**), NPPB (**c**,**d**), Niflumic acid (**e**,**f)**, or Nicardipine (**g**,**h**) for 2 days had no observable effect on *D. japonica* morphology.

Supplemental Tables

Table S2. Data statistics for RNA-seq, Related to Figure 2 and Tables 1 and 3. The 40 bp single end reads generated by Illumina HiSeq 2500 were quality checked and processed to remove the low quality bases and the adapter contamination. The table below lists the data generated for the individual samples.

Sample name	Chemistry	Barcode sequences	Total number of reads generated Post-processing (in millions)
WildType Head 2	40*1	TS13-AGTCAA	33.67
WildType Head 1	40*1	TS12-CTTGTA	39.18
BaCl2 Head 2	40*1	TS11-GGCTAC	36.72
BaCl2 Head 1	40*1	TS10-TAGCTT	34.64

Table S3. Alignment statistics for RNA-seq experiments, Related to Figure 2 and Tables 1 and 3. As the gene feature file for *Dugesia japonica* is not available, the reads were aligned to the *Dugesia japonica* (complete CDS regions) taken from NCBI (https://www.ncbi.nlm.nih.gov/nuccore/? term=Dugesia%20japonica) which consists of 138,026 nucleotide sequences, downloaded from the NCBI database using Tophat. The table below shows the alignment percentage of the reads mapped to the reference.

Sample name	No of reads (in millions)	Alignment percentage
WildType Head 2	33.67	92.60%
WildType Head 1	39.18	94.30%
BaCl2 Head 2	36.72	93.90%
BaCl2 Head 1	34.64	96.20%

Table S4. Gene Ontology Analysis, Related to Figure 2 and Tables 1 and 3. Most significant gene ontology categories affected at the transcript level with $BaCl_2$. All data for gene ontology can be found in Table S5.

Go Term Theme	***Category***	***Frequency***	***PAGE Z-Score***	***PAGE Raw p-value***	***FDR***
Biological Process	translation [go:0006412]	96	6.602042	4.06E-11	5.72E-09
	intracellular protein transport [go:0006886]	53	2.867622	0.004136	0.291566
	cell cycle [go:0007049]	17	-2.63838	0.00833	0.391526
	tricarboxylic acid cycle [go:0006099]	21	2.35727	0.01841	0.439486
	transmembrane receptor protein tyrosine kinase signaling pathway	5	2.270731	0.023163	0.439486
	pyrimidine nucleotide biosynthetic process [go:0006221]	5	2.248818	0.024524	0.439486
	protein glycosylation [go:0006486]	29	2.239905	0.025097	0.439486
	dna recombination [go:0006310]	8	-2.21806	0.026551	0.439486
	de novo' pyrimidine nucleobase biosynthetic process [go:0006207]	6	2.196554	0.028052	0.439486
	dna integration [go:0015074]	20	-2.14806	0.031709	0.447092
	malate metabolic process [go:0006108]	6	-2.03848	0.041502	0.492306
	vesicle-mediated transport [go:0016192]	35	1.986827	0.046942	0.492306
Molecular Function	structural constituent of cytoskeleton [go:0005200]	89	-7.40681	1.29E-13	2.69E-11
	structural constituent of ribosome [go:0003735]	100	6.812948	9.56E-12	9.94E-10
	acyl-coa dehydrogenase activity [go:0003995]	9	3.133764	0.001726	0.119655
	nad-dependent histone deacetylase activity (h3-k14 specific)	7	3.026156	0.002477	0.128796
	nad+ kinase activity [go:0003951]	7	2.825761	0.004717	0.196221

	proton-transporting atp synthase activity, rotational mechanism	7	2.604398	0.009204	0.275972
	protein tyrosine phosphatase activity [go:0004725]	38	-2.54166	0.011033	0.275972
	nucleotidyltransferase activity [go:0016779]	12	2.513792	0.011944	0.275972
	microtubule binding [go:0008017]	39	-2.45754	0.013989	0.275972
	mannosyl-oligosaccharide 1,2-alpha-mannosidase activity	8	2.449566	0.014303	0.275972
	extracellular matrix structural constituent [go:0005201]	16	-2.43919	0.01472	0.275972
	flavin adenine dinucleotide binding [go:0050660]	27	2.410711	0.015921	0.275972
	histone-lysine n-methyltransferase activity [go:0018024]	14	2.330139	0.019799	0.297096
	inorganic anion exchanger activity [go:0005452]	7	2.326406	0.019997	0.297096
	carboxypeptidase activity [go:0004180]	7	2.091671	0.036468	0.425427
	peptidyl-dipeptidase activity [go:0008241]	7	2.091671	0.036468	0.425427
	chromatin binding [go:0003682]	9	2.068059	0.038634	0.425427
	ubiquitin-protein transferase activity [go:0004842]	48	2.020134	0.043369	0.425427
	phospholipid binding [go:0005543]	6	1.997395	0.045782	0.425427
	carbohydrate binding [go:0030246]	16	1.970462	0.048785	0.425427
Cellular Component	ribosome [go:0005840]	83	5.158659	2.49E-07	1.77E-05
	small ribosomal subunit [go:0015935]	9	3.061898	0.002199	0.078078
	cytosol [go:0005829]	11	2.920361	0.003496	0.082745
	nucleolus [go:0005730]	21	-2.30831	0.020982	0.346204
	large ribosomal subunit [go:0015934]	10	2.206271	0.027365	0.346204

	extracellular space [go:0005615]	15	2.180011	0.029257	0.346204
	motile cilium [go:0031514]	7	-2.04248	0.041104	0.416915

Table S6. Lists of genes depicted in Figure 2A and B, Related to Figure 2. (**A**) Full list of altered anion transport-related genes shown in Figure 2A. (**B**) Full list of altered transmission of nerve impulse-related genes shown in Figure 2C.

Table 6A

Name	***Probe Value***	***Description***
ABCA1	1.0018	ATP-binding cassette, sub-family A (ABC1), member 1
SLC12A2	0.3578	solute carrier family 12 (sodium/potassium/chloride transporters), member 2
SLC26A3	-2.0998	solute carrier family 26 (anion exchanger), member 3
SLC4A3	0.0388	solute carrier family 4, anion exchanger, member 3
SLC26A4	-1.201	solute carrier family 26, member 4
SLC17A1	10.9346	solute carrier family 17 (organic anion transporter), member 1
SLC22A11	3.5889	solute carrier family 22 (organic anion/urate transporter), member 11
ABCC3	1.3558	ATP-binding cassette, sub-family C (CFTR/MRP), member 3
SLCO1A2	-1.2222	solute carrier organic anion transporter family, member 1A2
ABCC2	-0.4388	ATP-binding cassette, sub-family C (CFTR/MRP), member 2
ABCC1	-0.896	ATP-binding cassette, sub-family C (CFTR/MRP), member 1
SLC22A6	-1.1533	solute carrier family 22 (organic anion transporter), member 6
ABCB1	-0.896	ATP-binding cassette, sub-family B (MDR/TAP), member 1
CAT	0.4148	catalase
UCP1	-0.2243	uncoupling protein 1 (mitochondrial, proton carrier)
TSPO	0.6788	translocator protein (18kDa)
m_Slco1a1	-1.2222	solute carrier organic anion transporter family, member 1a1

Table 6B

Name	**Probe Value**	**Description**
CTNNB1	-3.0765	catenin (cadherin-associated protein), beta 1, 88kDa
SLC8A1	1.8271	solute carrier family 8 (sodium/calcium exchanger), member 1

SLC12A2	0.3578	solute carrier family 12 (sodium/potassium/chloride transporters), member 2
SLC4A3	0.0388	solute carrier family 4, anion exchanger, member 3
GRIA2	0.3083	glutamate receptor, ionotropic, AMPA 2
GRIK2	2.546	glutamate receptor, ionotropic, kainate 2
TRPC3	0.5344	transient receptor potential cation channel, subfamily C, member 3
ASIC5	2.4432	acid-sensing (proton-gated) ion channel family member 5
P2RX4	0.8279	purinergic receptor P2X, ligand-gated ion channel, 4
CACNA2D1	1.3416	calcium channel, voltage-dependent, alpha 2/delta subunit 1
KCNA3	0.8759	potassium voltage-gated channel, shaker-related subfamily, member 3
KCNC2	-1.0571	potassium voltage-gated channel, Shaw-related subfamily, member 2
KCNH2	0.7843	potassium voltage-gated channel, subfamily H (eag-related), member 2
CAT	0.4148	catalase
FAAH	-0.8367	fatty acid amide hydrolase
GLUL	-1.415	glutamate-ammonia ligase
NPR1	0.6392	natriuretic peptide receptor A/guanylate cyclase A (atrionatriuretic peptide receptor A)
DAO	1.1035	D-amino-acid oxidase
ERG	1.5128	v-ets erythroblastosis virus E26 oncogene homolog (avian)
FOS	-0.2607	FBJ murine osteosarcoma viral oncogene homolog
JUN	0.3939	jun proto-oncogene
REST	-0.1284	RE1-silencing transcription factor
EGFR	1.2985	epidermal growth factor receptor
MEN1	-1.3847	multiple endocrine neoplasia I
MARK2	-1.9312	MAP/microtubule affinity-regulating kinase 2
UBC	0.2766	ubiquitin C
RANBP2	-0.375	RAN binding protein 2
CAV1	-1.0436	caveolin 1, caveolae protein, 22kDa
SNAP25	-0.228	synaptosomal-associated protein, 25kDa
ANK2	1.1996	ankyrin 2, neuronal
KIF5B	-0.1274	kinesin family member 5B
PANX1	-3.5446	pannexin 1
AGRN	-1.2874	agrin
GFAP	1.8981	glial fibrillary acidic protein
NALCN	0.8476	sodium leak channel, non-selective
INS	1.5798	insulin
NTN1	1.616	netrin 1
TNF	-0.25	tumor necrosis factor
CDC42	-0.2927	cell division cycle 42 (GTP binding protein)
RAC1	0.0752	ras-related C3 botulinum toxin substrate 1 (rho family, small GTP binding protein Rac1)

RAP1B	0.6267	RAP1B, member of RAS oncogene family
RASGRF1	-0.9149	Ras protein-specific guanine nucleotide-releasing factor 1
MYLK	1.7125	myosin light chain kinase
CASP3	-0.7907	caspase 3, apoptosis-related cysteine peptidase
GPER1	0.3777	G protein-coupled estrogen receptor 1
NPY1R	85.4924	neuropeptide Y receptor Y1
CXCR4	85.4924	chemokine (C-X-C motif) receptor 4
MMP9	3.4586	matrix metallopeptidase 9 (gelatinase B, 92kDa gelatinase, 92kDa type IV collagenase)
CDK5	-0.2833	cyclin-dependent kinase 5
BRSK2	-0.8513	BR serine/threonine kinase 2
RAB8A	2.13	RAB8A, member RAS oncogene family
RAB10	0.0681	RAB10, member RAS oncogene family
APC	1.0329	adenomatous polyposis coli
PICK1	1.3926	protein interacting with PRKCA 1
ACE	0.9108	angiotensin I converting enzyme (peptidyl-dipeptidase A) 1
PRMT1	-0.1001	protein arginine methyltransferase 1
DBI	-0.085	diazepam binding inhibitor (GABA receptor modulator, acyl-Coenzyme A binding protein)
TSPO	0.6788	translocator protein (18kDa)
MSRA	-1.1203	methionine sulfoxide reductase A
PITPNA	-0.3698	phosphatidylinositol transfer protein, alpha
GRIK1	-3.1039	glutamate receptor, ionotropic, kainate 1

Transparent Methods

Planarian care

A clonal strain of *Dugesia japonica* was maintained at 13 °C in Poland Spring water with weekly feedings of liver paste and twice-weekly water changes, as in (Oviedo et al., 2008a). Worms were maintained at 13°C for the duration of the experiment in order to prevent spontaneous fissioning, which occurs at a greater rate at higher temperatures and which would interfere with interpretation of results regarding timing of regeneration (Oviedo et al., 2008a). Due to experimental temperature being 13°C, worms were taken from a cold-adapted 13 °C colony which is continuously maintained at that temperature. Worms were starved for at least one week prior to the beginning of each experiment.

$BaCl_2$ Adaptation and Loss of Adaptation

Whole worms were maintained at 13 °C in untreated tissue culture plates containing either Poland Spring water or 1 mM $BaCl_2$ (MP Biomedicals Inc) in Poland Spring water ($BaCl_2$ solution). Both water and $BaCl_2$ solutions were replaced once a week. A maximum of 30 worms were kept in each plate (diameter 100 mm), which contained approximately 50 mL of solution. Progression of response to $BaCl_2$ was assessed by regular examination of animals using a stereoscope. Worms that had fully regenerated in refreshed $BaCl_2$ for at least three weeks and were indistinguishable in appearance from untreated worms were designated "$BaCl_2$-adapted worms."

To assess the persistence of the $BaCl_2$ adaptation, $BaCl_2$-adapted worms were removed from the 1mM $BaCl_2$ solution and maintained in untreated tissue culture plates at 13 °C in Poland Spring water for 30 days before being placed again in 1mM $BaCl_2$ solution.

Drug treatments: $BaCl_2$ and ion channel blockers

In order to test the effects of particular channels on $BaCl_2$ adaptation, planaria were exposed to 1mM $BaCl_2$ in the presence of drugs that modify channels. In each case, planaria were exposed to either $BaCl_2$+treatment solution (Poland Spring water with 1 mM $BaCl_2$ and the respective drug) as well as 3 control solutions. Control solutions were Poland Spring water plus matching concentration of DMSO, drug control solution (Poland Spring water plus the drug (dissolved in DMSO)), or BaCl2-control solution (Poland Spring water, 1mM BaCl, and matching DMSO concentration). DMSO concentration never exceeded .1% as higher concentrations have been shown to interfere with normal planarian function (Pagan et al., 2006, Stevens et al., 2015, Yuan et al., 2012). Worms were maintained in tissue culture treated dishes at 13 °C. Multiple concentrations were tested for each drug, and the lowest effective concentration was used for each.

Bromocriptine mesylate at a final concentration of 0.5 μM (Tocris #0427), dissolved in Poland Spring from a stock dissolved in DMSO (final DMSO concentration: 0.0075%) was used to block monoamines. Inhibition of calcium activated chloride channels was performed using 5.0 μM 5-Nitro-2-(3-phenylpropylamino)benzoic acid (NPPB, Cayman Chemical #17292) or 1.25 μM niflumic acid (Tocris #4112) in Poland Spring from a stock dissolved in DMSO (final DMSO concentration 0.006% or 0.000726%, respectively). Inhibition of calcium channels was performed using 2.5 μM nicardipine hydrochloride (Sigma-Aldrich #N7510) in Poland Spring from a stock dissolved in DMSO (final concentration of DMSO 0.0025%). Inhibition of TRPM was achieved using 100 μM AMTB hydrochloride (Tocris #3989) in Poland Spring from a stock dissolved in DMSO (final concentration of DMSO 0.1%). For AMTB treatments, media was refreshed once a week, all other solutions were refreshed every two days.

Visualization of relative membrane potentials with $DiBAC_4(3)$ dye imaging

$DiBAC_4(3)$ (bis-(1,3-dibutylbarbituric acid)-trimethine oxanol) (Invitrogen) was used as previously described (Oviedo et al., 2008b). Briefly, a stock solution (1.9 mM) was diluted 1:1000 (1.9 µM) in Poland Spring water or 1 mM $BaCl_2$ solution, and worms were soaked in the $DiBAC_4(3)$ solution for >30 minutes before imaging. Worms were then immobilized in 2% low-meting point agarose, using custom-fabricated Planarian Immobilization Chips as per Dexter and colleagues (Dexter et al., 2014). Images of the ventral side of immobilized planaria were captured with the Nikon AZ100 Stereomicroscope using epifluorescence optics and NIS-Elements imaging software. Treatment and control animals were captured within the same frame and care was taken to ensure that planaria did not move during image acquisition. No data points or image features were removed from our analysis. To quantify differences in relative depolarization, average pixel intensity of the head region, defined as the anterior $1/6^{th}$ of the worm, was quantified with ImageJ, after flat-field correction. This treatment avoided confounding the analysis by including fluorescence due to background and slime.

RNA extraction and RNA-seq

Total RNA was extracted from wild type and $BaCl_2$-adapted *D. japonica* heads. Two biological replicates were collected for each treatment, with 25 worms pooled per replicate. Worms were kept in 1 mM $BaCl_2$ for 35 days, when $BaCl_2$-insensitive heads had fully regenerated. Heads (as defined by the anterior $1/6^{th}$ of the worm) were then amputated and RNA was extracted using Trizol (Ambion/ThermoFisher) as per the manufacturer's instructions. RNA was pelleted via isopropanol extraction and then suspended in 80% ethanol. Following DNase-treatment, the concentration of RNA was crudely quantified via NanoDrop™, and samples were stored at -80°C. Samples were sent to the Whitehead Institute Genome Technology Core for sequencing. Quality control for RNA was conducted using an Agilent 2100 Bioanalyzer. While RIN scores cannot be used with planarian species due to an absence of 28s rRNA peaks (Kim, 2019, Liu and Rink, 2018), we confirmed quality of RNA prior to library prep with the sequencing core. Library prep was performed on high quality RNA using the TruSeq PolyA kit (Illumina) as per manufacturer's protocol. All sequencing libraries were then quantified, pooled and sequenced at single-end 40 base-pair using the Illumina HiSeq 2500. Following sequencing, data processing was done using the standard Illumina pipeline and Fastq files were generated for data processing and assembly.

Data Processing and Assembly

Raw Illumina files were processed by Genotypic Technology Ltd. (Bangalore, India) for read mapping and the identification of differentially expressed transcripts. Raw data were downloaded and processed (Adapter, B-block and low-quality base filtering) using Genotypic's proprietary Perl script for removing adapter and low-quality base trimming. RNA-Seq reads were then mapped using the ultra-high-throughput short read aligner Bowtie (Langmead, 2010) and reference alignment was conducted with TopHat-2.0.13 (Trapnell et al., 2009), a fast splice junction mapper for RNA-Seq reads. Processed data were inputted into TopHat and default parameters for directional libraries were used. Cufflinks-2.2.1 was used to assemble transcripts and to identify transcripts that were differentially expressed using default settings and -G option to facilitate read mapping. Biological replicates were combined using Cuffmerge and then analyzed using CuffDiff (2.2.1) for replicate samples by modeling the variance in fragment counts across replicates as a function of the mean fragment count. Each replicated condition was first used to build a model. Models were generated from each biological replicate and were averaged to provide a single global model for all conditions in the experiment. Cuffdiff was then used

to determine significant changes in transcript levels. Data and alignment statistics for the Illumina runs are presented in Tables S2 and S3.

Expression level estimation was reported as fragments per kilobase of transcript sequence per million mapped fragments (FPKM) value together with confidence intervals. The false discovery rate or FDR-adjusted p-value of the test statistic (q-value) was also generated. An in-house pipeline was developed to automate the abovementioned mapping and assembly process. All transcripts were annotated for Gene Ontology (GO) by performing a blast alignment. The 138,026 transcript sequences of *D. japonica* were subjected to blast against the 385,255 sequences of Platyhelminthes database extracted from Uniprot as a reference. Table S1 contains all processed transcript data, including fold change and p-value.

Pathway Studio 10.0 (Elsevier) and ResNet 11.0 were used for sub-network enrichment analysis (SNEA) of cell processes. The option of "best p value, highest magnitude fold change" in Pathway Studio was used for duplicated probes. Transcripts were successfully mapped using Name and Alias. SNEA was performed to identify gene networks that were significantly different in the treatment samples compared to control. A Kolmogorov–Smirnov test with 1000 permutations was conducted to determine whether specific networks were preferentially regulated compared to the background reference probability distribution. Networks were constructed based on common regulators of expression and regulators of specific cell processes. The enrichment p-value for a gene seed was set at $p< 0.05$. Additional details on the use of SNEA can be found in (Langlois and Martyniuk, 2013).

qPCR

1 µg total RNA extracted from the anterior 1/6th of *Dugesia japonica* was DNase treated and used as a template to synthesize cDNA (iScript gDNA Clear cDNA Synthesis Kit, BioRad, USA). PCR primers for Dj-TRPMa were obtained from the Agata lab (Inoue et al., 2014). Slc2a1 primers (F: 5'-TTGAACGATTCCGACCGCA-3', R: 5'-GGGTTTGCTTTGGGACTAGGA-3') were designed based on the upregulated sequences identified in the RNAseq analysis and were validated using melt curve analysis. GAPDH (Takano et al., 2007) was used as the reference gene. For qPCR, each 10 µL reaction was run in duplicate and contained: 5 µL of 2x PowerUp SYBR Green Master Mix (Applied Biosystems, USA), 0.5 µL of 10 µM of forward and reverse gene-specific primers, and 1.33 µL of diluted (1:20 for Slc2a1, 1:5 for Dj-TRPMa) cDNA template. qPCR was performed using the Step One Plus Real Time System (Applied Biosystems, USA) according to manufacturer's instructions. Relative expression was analyzed using the Pfaffl method (Pfaffl, 2001).

Data and Software Availability

RNA-Seq unprocessed data has been deposited in the National Center for Biotechnology Information (NCBI) Gene Expression Omnibus (GEO) and is accessible through GEO Series accession number (GSE98084).

Supplemental References

DEXTER, J. P., TAMME, M. B., LIND, C. H. & COLLINS, E. M. 2014. On-chip immobilization of planarians for in vivo imaging. *Scientific reports,* 4**,** 6388.

INOUE, T., YAMASHITA, T. & AGATA, K. 2014. Thermosensory signaling by TRPM is processed by brain serotonergic neurons to produce planarian thermotaxis. *J Neurosci,* 34**,** 15701-14.

KIM, I. V., ROSS, ERIC J., DIETRICH, SASCHA, DÖRING, KRISTINA, ALVARADO, ALEJANDRO SÁNCHEZ, KUHN, CLAUS-D. 2019. Efficient depletion of ribosomal RNA for RNA sequencing in planarians. *bioRxiv,* 670604.

LANGLOIS, V. S. & MARTYNIUK, C. J. 2013. Genome wide analysis of Silurana (Xenopus) tropicalis development reveals dynamic expression using network enrichment analysis. *Mechanisms of development,* 130**,** 304-22.

LANGMEAD, B. 2010. Aligning short sequencing reads with Bowtie. *Curr Protoc Bioinformatics,* Chapter 11**,** Unit 11 7.

LIU, S.-Y. & RINK, J. C. 2018. Total RNA Isolation from Planarian Tissues. *In:* RINK, J. C. (ed.) *Planarian Regeneration: Methods and Protocols.* New York, NY: Springer New York.

OVIEDO, N. J., NICOLAS, C. L., ADAMS, D. S. & LEVIN, M. 2008a. Establishing and maintaining a colony of planarians. *CSH Protoc.,* 2008**,** db.prot5053.

OVIEDO, N. J., NICOLAS, C. L., ADAMS, D. S. & LEVIN, M. 2008b. Live Imaging of Planarian Membrane Potential Using DiBAC4(3). *Cold Spring Harb Protoc,* 2008**,** pdb.prot5055-.

PAGAN, O. R., ROWLANDS, A. L. & URBAN, K. R. 2006. Toxicity and behavioral effects of dimethylsulfoxide in planaria. *Neurosci Lett,* 407**,** 274-8.

PFAFFL, M. W. 2001. A new mathematical model for relative quantification in real-time RT-PCR. *Nucleic Acids Res,* 29**,** e45.

STEVENS, A. S., PIROTTE, N., PLUSQUIN, M., WILLEMS, M., NEYENS, T., ARTOIS, T. & SMEETS, K. 2015. Toxicity profiles and solvent-toxicant interference in the planarian Schmidtea mediterranea after dimethylsulfoxide (DMSO) exposure. *J Appl Toxicol,* 35**,** 319-26.

TAKANO, T., PULVERS, J. N., INOUE, T., TARUI, H., SAKAMOTO, H., AGATA, K. & UMESONO, Y. 2007. Regeneration-dependent conditional gene knockdown (Readyknock) in planarian: demonstration of requirement for Djsnap-25 expression in the brain for negative phototactic behavior. *Dev Growth Differ,* 49**,** 383-94.

TRAPNELL, C., PACHTER, L. & SALZBERG, S. L. 2009. TopHat: discovering splice junctions with RNA-Seq. *Bioinformatics,* 25**,** 1105-11.

YUAN, Z., ZHAO, B. & ZHANG, Y. 2012. Effects of dimethylsulfoxide on behavior and antioxidant enzymes response of planarian Dugesia japonica. *Toxicol Ind Health,* 28**,** 449-57.